ISSN 1063-7729, Astronomy Reports, 2007, Vol. 51, No. 1, pp. 1–18. © Pleiades Publishing, Ltd., 2007.
Original Russian Text © A.S. Gusev, 2007, published in Astronomicheskiĭ Zhurnal, 2007, Vol. 84, No. 1, pp. 1–21.

Properties of Galactic Disks at Optical and Near-IR Wavelengths

A. S. Gusev

Sternberg Astronomical Institute, Moscow State University,
Universitetskiĭ pr. 13, Moscow, 119899 Russia

Received April 10, 2006; in final form, July 7, 2006

Abstract—We have analyzed the radial scales, central surface brightnesses, and colors of 400 disks of various types of galaxies. For nine galaxies, the brightness decrease and the central disk brightness were obtained via a two-dimensional decomposition of the $UBVRIJHK$ photometric images into bulge and disk componens. We used published disk parameters for 392 of the galaxies. The central surface brightness $\mu^0_{0,i}$ and linear (disk) scale length h vary smoothly along the Hubble sequence of galaxies within a rather narrow interval. The disks of relatively early-type galaxies display higher central K surface brightnesses, higher central surface densities, higher central mass-to-luminosity ratios $M/L(B)$, smaller sizes (relative to the diameter of the galaxy D_{25}), redder integrated colors, and redder central colors. The color gradient normalized to the radius of the galaxy and the "blue" central surface brightness of the disk, $\mu^0_{0,i}(B)$, are both independent of the galaxy type. The radial disk scales in different photometric bands differ less in early-type than in late-type galaxies. A correlation between the central disk surface brightness and the total luminosity of the galaxy is observed. We also consider the influence of dust on the photometric parameters of the disks.

PACS numbers : 98.52.Nr, 98.62.Hr, 98.62.Js, 95.75.De, 98.62.Lv
DOI: 10.1134/S1063772907010015

1. INTRODUCTION

Knowledge of the photometric parameters of disk components of galaxies is essential for studies of the dynamics and evolution of galaxies, dark matter, and the distribution of dust in galaxies. In the classical case of a thin exponential disk ($I = I_0 \exp(-r/h)$ or $\mu = \mu_0 + 1.086(r/h)$, where $I(r) = -2.5 \log \mu(r) + C$ is the radial brightness profile, the disk is described by two parameters in each photometric band: the (disk) scale length h and the central surface brightness μ_0. Various combinations of photometric parameters can be used to determine the radial color gradients (which depend on the age and chemical composition of the stellar population of the disk and the distribution of dust), and to estimate the distribution of the stellar mass and the central surface density of the disk.

In numerous studies of the properties of galactic disks (see the review below), either galaxies with narrowly specified properties (e.g., only Sb galaxies [1], E–S0 galaxies [2], galaxies observed "face-on" [3], very inclined galaxies [4]) were considered, or a decomposition was carried out using no more than a few (usually, one) photometric bands. Six-color $BVRJHK$ photometry was carried out in [3], and five-color photometry in the two studies [4] ($BVRIJK$) and [5] ($UBVRI$). This substantially reduces opportunities for analyzing the photometric parameters of the disks (for example, the absence of IR photometric data makes it impossible to determine the influence of dust on the photometric properties of a disk). Note also that, in most studies, a one-dimensional decomposition was based on radial profiles of the galaxies, which can in some cases result in incorrect values for the disk and bulge parameters [6].

The photometric properties of disks in the optical and IR are essential for a number of important problems, both fundamental and applied. Examples of the former include the formation and evolution of disks in S0 galaxies. Several possible mechanisms for the rapid depletion of gas in lenticular galaxies, leading to an absence of spiral arms and appreciable star formation, have been discussed. The photometric properties of the disks of spiral and S0 galaxies ("cleaned" of the bulge radiation in lenticular and of the spiral-arm radiation in spiral galaxies) can help us determine the differences between them.

An important applied problem is determining the mass distributions in galaxies as a whole, and in their disks in particular. This problem is currently being addressed using two-dimensional spectroscopic observations. However, there are two difficulties with this approach. First, such observations require large telescopes and special detectors. Second, decomposition of the mass distribution into spherical and flat components requires knowledge of the distribution of

the radiation in the disk and bulge of the galaxy. In general, the surface density is proportional to the surface brightness of the old stellar population corrected for absorption by dust. In a first approximation, it is assumed that the mass distribution corresponds to the radiation distribution in the K-band. However, IR observations currently much more complicated (and rarer) than B, V, R, and I observations. Unfortunately, the data from the 2MASS Catalog (JHK photometry) cannot be used to study the weak outer regions of galaxies. We have attempted to establish a relationship between the radiation distributions (disk scales) in optical bands and in the IR.

Here, we use a sample of 401 galaxies with various morphological types and wide ranges of disk inclinations and galaxy luminosities to study the dependence of the photometric parameters of the disks on the morphological type of the galaxy, radial variations of the disk color indices, the influence of dust on the photometric parameters of the disks, and the dependence of the observed scale for the radial brightness decrease on the disk inclination. We also estimate the surface density and mass-to-luminosity ratio for a disk in the center of a galaxy.

In one of the first studies in which the disk scale lengths were considered in more than one filter, Elmegreen and Elmegreen [7] carried out one-dimensional decompositions and analyzed 34 weakly inclined spiral (Sb–Sd) galaxies without bars in the B and I bands; the average ratio of the disk scales in these bands was $\langle h(B)/h(I)\rangle = 1.16$.

Peletier et al. [8] studied the properties of the disks in 37 Sb–Sd galaxies with various inclinations via a one-dimensional decomposition into bulge and disk components in B, R, and K. The resulting average ratio of disk scales $h(B)/h(K)$ was 1.32 (with values ranging from one to two), and increased with the ellipticity of the disk isophotes (inclination). For S0 galaxies, $\langle h(B)/h(I)\rangle = 1.04 \pm 0.05$ [9], substantially lower than the $h(B)/h(I)$ ratio for spiral galaxies [8]. According to [8], the central disk K surface brightness and $B-K$ color index are related: brighter central regions are redder. As a consequence, Peletier et al. [8] suggested that the centers of galactic disks are optically thick in the B band, but optically thin in the K band. They estimated that a radial variation of the age and metallicity of the stellar population in the absence of an appreciable influence from dust would yield $h(B)/h(K) \approx 1.1$–1.2.

To determine the impact of dust on the photometric parameters of disks, Cunow [1] studied 14 Sb galaxies with various inclinations in the $BVRI$ bands using one-dimensional decompositions. She found that the disk scale ratios in the various filters increase with the isophote ellipticity e ($e \equiv 1 - b/a$): $h(B)/h(I)$, $h(V)/h(I)$, and $h(R)/h(I)$ increase from 1.0 for disks with $e = 0$ to 1.8, 1.5, and 1.3, respectively, for disks with $e > 0.8$. Cunow [1] suggests that this indicates a dominant role by dust (compared to the age and chemical composition of the stellar population) in determining the ratios of the disk scale lengths in different photometric bands.

Having extended the sample to 60 Sa–Sbc galaxies (28 of which display signs of core activity), Cunow [10] detected a difference between the dependences of $h(B)/h(I)$, $h(V)/h(I)$, and $h(R)/h(I)$ on the ellipticity e for active and normal galaxies. In active galaxies, the ratios $h(B)/h(I)$, $h(V)/h(I)$, and $h(R)/h(I)$ were all found to be equal to 1.0, independent of the galaxy inclination, while the results for normal galaxies confirmed the data of [1]. According to [10], for normal galaxies, the average disk brightness-decrease scale ratios are $\langle h(B)/h(I)\rangle = 1.30 \pm 0.04$, $\langle h(V)/h(I)\rangle = 1.14 \pm 0.03$, and $\langle h(R)/h(I)\rangle = 1.10 \pm 0.02$. Modeling of the influence of dust on the photometric properties of the disks showed that the dust optical depth at the center of the galaxy is $\tau_0(B) = 3^m \pm 2^m$ for normal galaxies and $\tau_0(B) = 0^m \pm 2^m$ for active galaxies, while the ratio of the scales for the decreases in the dust surface density and the B-band brightness is $h_\tau/h(I) = 0.96$ for both normal and active galaxies. Analysis of the dependence of $h(B)/h(I)$ on the absolute magnitude of the galaxy $M(B)$ and the linear scale length for the disk $h(I)$ showed that $h(B)/h(I)$ does not depend on $M(B)$, although a weak correlation is observed for normal galaxies: $h(B)/h(I) \approx h(I)/20 + 1$, where $h(I)$ is measured in kpc.

Van Driel et al. [11] studied 27 galaxies at far FIR wavelengths (50 and 100 μm), and demonstrated that the galactic centers were optically thick in the B band, $\tau_0(B) = 4$. "Warm" and "cold" dust in have different distributions in the galaxies: $h(100\ \mu\text{m})/h(50\ \mu\text{m}) = 1.21$, while $h(B)/h(100\ \mu\text{m}) = 1.12$ and $h(B)/h(50\ \mu\text{m}) = 1.36$.

The properties of 27 Seyfert galaxies with various inclinations were studied in [12]. The disk parameters were obtained from VRI photometry via one-dimensional decomposition of the radiation. It was found that the central surface brightness of a disk decreases with increasing disk size. According to [12], $\langle h(V)/h(I)\rangle = 1.25$ and $\langle h(R)/h(I)\rangle = 1.13$. This disagrees with the data of [10] for galaxies with nuclear activity.

MacArthur et al. [13] studied 172 galaxies of all morphological types with modest inclinations in B, V, R, and H via one-dimensional decomposition into bulge and disk components. One aim of this study was to determine the star-formation history in the disks, and gradients of the average age and metallicity

of the stellar population as a function of distance from the center. It was shown that there had not been any active star-formation bursts in the galactic disks outside the spiral arms, at least over the last one to two billion years. The average age and metallicity of the stellar population of the galactic disks increase from later to earlier morphological types. Both the age and metallicity are proportional to the central surface brightness of the disk and the IR luminosity of the galaxy, as well as to the maximum rotational velocity. The age of the disk is also weakly correlated with the radial scale of the disk. The average age and metallicity of the disk stellar population decrease with the distance from the center. The radial age gradient (in units of the disk scale) is correlated with the luminosity, size, and rotational velocity of a galaxy, and decreases from late to early type galaxies. No correlations were detected for the metallicity and age gradients as functions of linear distance. According to [13], dust does not contribute substantially to radial variations of the disk colors.

De Grijs [14] studied the properties of 46 galaxies with various morphological types and appreciable inclinations in the BIK filters via one-dimensional decompositions into bulge and disk components. He obtained for Sab and later-type galaxies, $\langle h(B)/h(I)\rangle = 1.36 \pm 0.18$, $\langle h(B)/h(K)\rangle = 1.65 \pm 0.41$, and $\langle h(I)/h(K)\rangle = 1.15 \pm 0.19$, with the range of values increasing from early- to late-type galaxies. For S0–Sa galaxies, $h(B)/h(I) \approx h(B)/h(K) \approx h(I)/h(K) \approx 1$, while, for Scd galaxies, the ranges of the scale ratios were $h(B)/h(I)$, $h(B)/h(K)$, and $h(I)/h(K)$ 1–1.8, 1–2.2, and 1–1.5, respectively. Note that, in the sample of galaxies [14], some other photometric parameters of the disk (in particular, the central surface brightness and the linear disk scale in the K band) are roughly constant for S0–Sa galaxies: $\mu_0(K) = 15^m$–16^m, $h(K) = 1$–2 kpc. In later-type galaxies, the range of the calculated $\mu_0(K)$ and $h(K)$ values increases from Sab to Sd galaxies. In Scd galaxies, $\mu_0(K) = 15^m$–18^m and $h(K) = 2$–7 kpc. According to the sample [14], the $B-I$, $B-K$, and $I-K$ integrated disk color indices are essentially independent of morphological type. The calculations of [14] indicate that, in the absence of an appreciably influence from dust, the ratio $h(B)/h(I)$ due to the radial metallicity gradient for the stellar population is equal to 1.17.

The properties of the disks and bulges of galaxies have recently begun to be studied using two-dimensional decompositions, making it possible to more correctly determine the photometric parameters of the bulges and disks (as well as other components, such as bars). Examples are the studies [2], based on R-band observations of 51 elliptical and lenticular galaxies, [5], based on the properties of 26 spiral galaxies with disk inclinations $i < 65°$ in the $UBVRI$ filters, [4], where seven edge-on Sb–Sc galaxies were analyzed in the $BVIJK$ bands, and [3], in which $BVRIHK$ photometric data for 86 face-on spiral galaxies were analyzed.

In his study of disk scales in various filters, Mollenhoff [5] showed that they decrease monotonically from $h(U)$ to $h(I)$ for each galaxy. However, the intervals of disk scales normalized to $h(I)$ are fairly broad: 1.0–1.5 for $h(U)/h(I)$, 1.0–1.4 for $h(B)/h(I)$, and so on. The integrated disk color indices decrease from Sa to Sc galaxies: $U-B$ from 0.2^m to -0.2^m, $B-V$ from 0.75^m to 0.5^m, $V-R$ from 0.45^m to 0.35^m, and $R-I$ from 0.85^m to 0.5^m.

The study [4] was devoted to the structure of the stellar and dust disks. It was shown that the ratio of the radial scales for the stellar and dust disks in the V band is $h_{disk}/h_{dust} = 0.7 \pm 0.1$, while the ratio of the vertical scales is $z_{disk}/z_{dust} = 1.8 \pm 0.6$; $h/z \sim 10$. Thus, the stellar disk seems to be thicker but less extended than the dust disk. The optical depth of the dust at the galactic center (along the polar axis) is $\tau_0(B) = 0.4$–1.0. This is in disagreement with the data of [8, 10, 11], which indicate that the dust disks are optically thick in B at the centers of the galaxies.

The study [3] basically confirms the results of [5, 7, 8]: on average, $h(B)/h(I) = 1.12$, $h(V)/h(I) = 1.04$, $h(R)/h(I) = 1.03$, $h(B)/h(H) = 1.18$, and $h(B)/h(K) = 1.22$ for face-on galaxies.

2. THE SAMPLE OF GALAXIES

For our study of the photometric parameters of disks in galaxies of various types, we used the data from [1–5, 7, 8, 10, 12–14] for 392 galaxies (B and I disk scales for 34 galaxies obtained in [7]; $BVRI$ scales and central disk surface brightness for 62 galaxies from [1, 10], in $BVRH$ for 47 galaxies from [13], in $UBVRI$ for 26 galaxies from [5], in R for 26 galaxies from [2], in $BVIJK$ for 6 galaxies from [4], in VRI for 22 galaxies from [12], in BRK for 37 galaxies from [8], in $BVRIHK$ for 86 galaxies from [3], and in BIK for 46 galaxies from [14], together with our previously obtained CCD photometry for 9 galaxies [6, 15–17]). When the selecting the data sources to be used, we gave priority to those in which the disk photometric parameters were studied in more than one photometric band (except for [2]). The integrated parameters of the galaxies (including the ellipticity e of the disk isophotes) were taken or calculated from data in the LEDA Catalog. We used the derived integrated parameters to determine the disk scale lengths h in kpc and the disk central surface brightness $\mu^0_{0,i}$ in mag/(sq. arcsec), corrected for the inclination of the galaxy. Thus, by using the available

Table 1. Basic data on the galaxies

Galaxy parameter	NGC number								
	524	532	783	1138	1589	2336	4136	5351	7280
Type	−1.2	2.0	5.1	−2.1	1.8	4.0	5.3	3.1	−1.0
$M_B^{0,i}$, mag	−21.63	−19.48	−21.14	−19.57	−21.73	−22.32	−18.41	−21.19	−19.41
D, Mpc	32.4	31.5	70.5	32.9	49.5	32.2	76.0	48.9	25.9
R_{25}, kpc	17.0	16.0	16.8	8.7	23.8	30.0	4.1	19.6	8.1
V_{rot}, km/s	300	191	46	25	323	256	93	202	131
e	0.05	0.74	0.25	0.05	0.63	0.42	0.18	0.53	0.36
$A_i(B)$, mag	0.00	0.49	0.30	0.00	0.54	0.39	0.06	0.39	0.00
M_{dust}, $10^6 M_\odot$	0.35	3.3	26	–	1.3	9.7	0.17	1.3	0.056

single-source data for the integrated parameters of the galaxies (taken from the LEDA database), we were able to decrease the dissimilarity of the sample objects.

In some cases, in addition to the overall sample of 392 galaxies, we considered a separate subsample containing the 144 galaxies studied in [2–5] via two-dimensional decompositions. We believe that the disk parameters determined in these studies are more reliable than those obtained via one-dimensional decompositions [6].

We also used our previous multi-color CCD photometry data of 9 galaxies. Information about the observations and processing for the $UBVRI$ photometry of NGC 2336 are given in [15], for the $BVRI$ photometry of NGC 4136 in [16], for the $BVRIJHK$ photometry of NGC 5351 in [17], and for the $UBVRIJHK$ photometry of NGC 524, NGC 532, NGC 783, NGC 1138, NGC 1589, and NGC 7280 in [6]. Additionally, we used the data from the 2MASS Catalog for NGC 2336 and NGC 4136 (images in the J, H, and K bands). A description of the data reduction for the 2MASS Catalog images is given in [6]; the technique used for the two-dimensional decompositions of the galactic radiation into bulge and disk components is presented in [6].

Table 1 presents the basic data for the 9 added-galaxies: the type, absolute magnitude $M_B^{0,i}$ corrected for absorption in the Galaxy and due to the disk inclination, distance to the galaxy D in Mpc, radius of the galaxy R_{25} in kpc determined from the 25^m/(sq. arcsec) B isophote, maximum rotational velocity V_{rot} in km/s corrected for the inclination, disk isophote ellipticity e, absorption $A_i(B)$ in B magnitudes due to the disk inclination, and mass of dust M_{dust} in solar masses. The galaxy types and $M_B^{0,i}$, V_{rot}, and $A_i(B)$ valyes were taken from LEDA electronic database. D and R_{25} were also obtained from LEDA Catalog (using a Hubble constant of $H_0 = 75$ km s^{-1} Mpc^{-1}). We obtained the e values for the galactic disks in [6, 15–17]. The data sources for M_{dust} for most galaxies and for V_{rot} for NGC 1138 are given in [6, 15]. The dusts masses for NGC 4136 and NGC 5351 were taken from [18] and [19], respectively.

Table 2 presents the disk photometric parameters for the 9 galaxies in the various filters. The columns of this table contain the (1) identification number of the galaxy, (2) filters used for the measurements, (3) disk scale lengths h in arcsec, with their errors, (4) central disk surface brightnesses μ_0 in mag/(sq. arcsec), corrected for absorption in the Galaxy, with their errors, (5) disk scale lengths h in kpc, with their errors, and (6) central disk surface brightnesses $\mu_{0,i}^0$ in mag/(sq. arcsec), with photometric (A_i) and geometrical (A_g) corrections for the inclination of the galaxy. The central surface brightnesses were corrected using the standard formula $\mu_{0,i} = \mu_0 - A_i - A_g$, where $A_g = 2.5\log(1-e)$. Columns 7–12 of the table are the same as columns 1–6.

3. ANALYSIS OF THE RESULTS

3.1. Central Surface Brightnesses and Color Indices of the Disks

In spite of the fact that the galaxies considered have a large range of luminosities ($L(B)_{\max} = 100L(B)_{\min}$) and sizes ($R_{25} = 2$–$40$ kpc), the central surface brightnesses of all the galactic disks $\mu_{0,i}^0$ lie in a fairly narrow interval, from 20.2^m/(sq. arcsec) to 22.7^m/(sq. arcsec) in B and from 16.9^m/(sq. arcsec) to 19.3^m/(sq. arcsec) in K (Fig. 1a and Table 3). The

Table 2. Photometric parameters of the galactic disks

NGC	Filter	h, arcsec	μ_0	h, kpc	$\mu^0_{0,i}$	NGC	Filter	h, arcsec	μ_0	h, kpc	$\mu^0_{0,i}$
524	U	35.9 ± 1.7	22.47 ± 0.06	5.65 ± 0.26	22.53	2336	U	99.6 ± 34.2	22.30 ± 0.07	15.55 ± 5.35	22.89
	B	27.4 ± 1.0	21.60 ± 0.06	4.31 ± 0.16	21.66		B	100.1 ± 1.5	21.92 ± 0.02	15.63 ± 0.24	22.51
	V	27.4 ± 1.0	20.58 ± 0.06	4.31 ± 0.16	20.64		V	82.9 ± 0.8	21.18 ± 0.01	12.94 ± 0.12	21.77
	R	27.5 ± 0.9	19.92 ± 0.06	4.32 ± 0.15	19.98		R	73.8 ± 0.6	20.63 ± 0.01	11.52 ± 0.09	21.22
	I	27.4 ± 0.8	19.14 ± 0.05	4.30 ± 0.12	19.20		I	72.3 ± 0.8	20.00 ± 0.02	11.29 ± 0.13	20.60
	J	27.3 ± 1.3	18.17 ± 0.08	4.29 ± 0.21	18.22		J	66.7 ± 1.9	18.88 ± 0.05	10.41 ± 0.29	19.47
	H	26.3 ± 1.3	17.39 ± 0.08	4.13 ± 0.21	17.45		H	75.0 ± 2.6	18.37 ± 0.05	11.71 ± 0.41	18.96
	K	26.9 ± 1.5	17.23 ± 0.09	4.23 ± 0.24	17.29		K	83.9 ± 3.4	18.33 ± 0.05	13.09 ± 0.53	18.92
532	U	36.0 ± 0.6	21.91 ± 0.03	5.49 ± 0.09	23.37	4136	–	–	–	–	–
	B	28.3 ± 0.1	21.11 ± 0.01	4.32 ± 0.02	22.57		B	40.4 ± 1.3	21.63 ± 0.05	1.50 ± 0.05	21.85
	V	27.6 ± 0.1	20.15 ± 0.01	4.21 ± 0.02	21.61		V	35.5 ± 1.0	20.84 ± 0.05	1.31 ± 0.04	21.06
	R	27.3 ± 0.1	19.55 ± 0.01	4.16 ± 0.01	21.02		R	33.5 ± 0.3	20.38 ± 0.02	1.24 ± 0.01	20.60
	I	28.1 ± 0.1	18.92 ± 0.01	4.29 ± 0.01	20.38		I	28.6 ± 1.2	19.57 ± 0.09	1.05 ± 0.04	19.79
	J	27.8 ± 0.6	17.94 ± 0.05	4.25 ± 0.09	19.40		J	29.4 ± 0.5	18.96 ± 0.02	1.08 ± 0.02	19.17
	H	28.0 ± 0.4	17.13 ± 0.03	4.28 ± 0.07	18.59		H	29.3 ± 1.0	18.33 ± 0.04	1.08 ± 0.04	18.55
	K	30.4 ± 0.5	17.00 ± 0.03	4.64 ± 0.07	18.46		K	27.4 ± 1.0	18.06 ± 0.04	1.01 ± 0.04	18.28
783	U	13.7 ± 2.2	21.25 ± 0.18	4.67 ± 0.74	21.56	5351	–	–	–	–	–
	B	13.2 ± 1.3	20.87 ± 0.11	4.51 ± 0.43	21.18		B	30.0 ± 0.4	21.81 ± 0.02	7.12 ± 0.09	22.63
	V	12.3 ± 0.8	19.99 ± 0.08	4.21 ± 0.26	20.31		V	28.5 ± 0.3	20.84 ± 0.03	6.76 ± 0.08	21.66
	R	11.9 ± 0.7	19.49 ± 0.08	4.07 ± 0.24	19.80		R	26.8 ± 0.2	20.30 ± 0.02	6.36 ± 0.05	21.12
	I	11.0 ± 0.3	18.79 ± 0.03	3.77 ± 0.11	19.11		I	27.4 ± 0.4	19.31 ± 0.03	6.51 ± 0.09	20.13
	J	11.4 ± 0.4	17.85 ± 0.05	3.89 ± 0.15	18.16		J	22.7 ± 0.2	18.20 ± 0.03	5.37 ± 0.06	19.02
	H	10.9 ± 0.4	17.10 ± 0.06	3.73 ± 0.15	17.41		H	22.1 ± 1.7	17.54 ± 0.20	5.23 ± 0.40	18.63
	K	10.7 ± 1.1	16.85 ± 0.14	3.66 ± 0.36	17.16		K	22.7 ± 0.4	17.23 ± 0.04	5.39 ± 0.10	18.05
1138	U	57.5 ± 41.9	23.16 ± 0.27	9.17 ± 6.69	23.22	7280	U	57.2 ± 3.5	22.85 ± 0.03	7.19 ± 0.45	23.33
	B	28.0 ± 1.4	22.85 ± 0.04	4.47 ± 0.23	22.90		B	37.1 ± 1.7	22.06 ± 0.03	4.65 ± 0.21	22.54
	V	23.6 ± 1.2	21.76 ± 0.05	3.76 ± 0.19	21.82		V	31.9 ± 1.6	21.02 ± 0.04	4.01 ± 0.20	21.51
	R	24.1 ± 1.0	21.14 ± 0.04	3.84 ± 0.16	21.19		R	30.6 ± 1.4	20.41 ± 0.04	3.85 ± 0.18	20.89
	I	26.1 ± 1.3	20.30 ± 0.05	4.16 ± 0.20	20.36		I	30.5 ± 1.1	19.70 ± 0.03	3.83 ± 0.14	20.19
	J	26.8 ± 1.5	19.30 ± 0.06	4.27 ± 0.23	19.35		J	33.7 ± 1.2	19.00 ± 0.04	4.23 ± 0.15	19.49
	H	26.5 ± 1.1	18.64 ± 0.05	4.23 ± 0.18	18.69		H	29.7 ± 0.7	18.28 ± 0.03	3.72 ± 0.09	18.77
	K	28.2 ± 2.5	18.53 ± 0.10	4.49 ± 0.39	18.58		K	33.0 ± 2.0	18.02 ± 0.07	4.14 ± 0.25	18.51
1589	U	33.9 ± 1.2	21.16 ± 0.03	8.14 ± 0.28	22.24						
	B	29.5 ± 0.6	20.61 ± 0.02	7.08 ± 0.14	21.68						
	V	28.1 ± 0.5	19.59 ± 0.02	6.74 ± 0.11	20.67						
	R	27.0 ± 0.4	19.00 ± 0.02	6.48 ± 0.10	20.08						
	I	27.2 ± 0.4	18.31 ± 0.02	6.52 ± 0.10	19.39						
	J	27.8 ± 1.0	17.30 ± 0.04	6.67 ± 0.25	18.38						
	H	24.9 ± 0.7	16.49 ± 0.04	5.99 ± 0.17	17.57						
	K	24.6 ± 0.7	16.24 ± 0.04	5.90 ± 0.17	17.32						

Table 3. Average central surface brightnesses and color indices of the disks

Filter or color index	Sample of 392 galaxies	Sample of 144 galaxies	Sample of 9 galaxies
X	$\mu^0_{0,i}(X)$		
U	21.14 ± 1.08	21.14 ± 1.08	22.74 ± 0.67
B	21.04 ± 0.86	21.32 ± 0.91	22.17 ± 0.59
V	20.57 ± 0.90	20.64 ± 0.87	21.23 ± 0.57
R	20.15 ± 0.92	20.31 ± 1.03	20.66 ± 0.56
I	19.75 ± 0.94	19.69 ± 0.96	19.90 ± 0.55
J	–	–	18.96 ± 0.55
H	18.02 ± 1.10	18.34 ± 1.25	18.26 ± 0.61
K	18.03 ± 1.13	18.17 ± 1.14	18.06 ± 0.65
$X-Y$	$(X-Y)^0_{0,i}$		
$U-B$	0.05 ± 0.20	0.05 ± 0.20	0.58 ± 0.24
$B-V$	0.42 ± 0.46	0.65 ± 0.26	0.94 ± 0.12
$V-R$	0.30 ± 0.31	0.44 ± 0.21	0.57 ± 0.06
$V-I$	1.02 ± 0.31	0.99 ± 0.28	1.32 ± 0.12
$J-H$	–	–	0.70 ± 0.10
$H-K$	0.15 ± 0.22	0.19 ± 0.32	0.20 ± 0.09
$B-H$	3.15 ± 0.59	2.97 ± 0.60	3.91 ± 0.33
$J-K$	–	–	0.90 ± 0.16
$X-Y$	$(X-Y)^{R_{25}}_{0,i}$		
$U-B$	-0.12 ± 0.60	-0.12 ± 0.60	-0.02 ± 0.38
$B-V$	0.39 ± 0.34	0.38 ± 0.37	0.69 ± 0.23
$V-R$	0.31 ± 0.50	0.37 ± 0.29	0.45 ± 0.16
$V-I$	0.72 ± 0.69	0.78 ± 0.39	1.13 ± 0.40
$J-H$	–	–	0.61 ± 0.16
$H-K$	0.18 ± 0.32	0.18 ± 0.32	0.28 ± 0.16
$B-H$	2.30 ± 0.66	2.32 ± 0.66	3.33 ± 0.64
$J-K$	–	–	0.89 ± 0.25

central disk surface brightnesses of the galaxies considered differ by no more than an order of magnitude. The graph in Fig. 1b shows an absence of any dependence between the central surface brightness $\mu^0_{0,i}$ corrected for the inclination and the disk inclination itself.

Let us consider the dependence between the central disk surface brightnesses in various photometric bands and the luminosity and type of the galaxy (Fig. 2). In spite of the large scatter in the corresponding plots, a correlation between $\mu^0_{0,i}$ and $M^{0,i}_B$ is observed, as well as a correlation between $\mu^0_{0,i}$ and the galaxy type in long-wavelength bands (Figs. 2c–2f). The luminosities and types of the galaxies in our sample are weakly correlated: since there are no bright Sd–Irr galaxies, it is difficult to determine which of the parameters (the luminosity or type) is influencing $\mu^0_{0,i}$. Considering the sample of 144 galaxies whose disk parameters were derived from two-dimensional decompositions, we found that the B, I, and K central disk surface brightnesses in the early-type galaxies (S0–Sc) are independent of $M^{0,i}_B$ and the morphological type (the correlation coefficient $|r| < 0.3$). We obtained the following dependences for the late-type spiral (starting from Sc) and irregular galaxies: $\mu_{0,i}(K) \sim (0.26 \pm 0.13)T + (0.54 \pm 0.14)M^{0,i}_B$ ($r = 0.7$), $\mu_{0,i}(I) \sim (0.24 \pm 0.13)T + (0.33 \pm 0.12)M^{0,i}_B$ ($r = 0.7$) and $\mu_{0,i}(B) \sim (0.28 \pm 0.11)T + (0.21 \pm 0.10)M^{0,i}_B$ ($r = 0.6$). Thus, the central disk surface brightnesses in the late-type galaxies increase with the integrated luminosity. This refers to the dependence between $\mu^0_{0,i}$ and the morphological type. Considering the galaxies of all morphological types, we obtained the dependences $\mu_{0,i}(K) \sim (0.16 \pm 0.06)T$ ($r = 0.45$) and $\mu_{0,i}(I) \sim (0.13 \pm 0.05)T$ ($r = 0.33$). $\mu_{0,i}(B)$ is independent of the galaxy type (Figs. 2a, 2c, 2e). Thus, on average, the central red brightness of the disk decreases from earlier to later galaxy type, while the central blue brightness remains constant for galaxies of all morphological types (Figs. 2a, 2c, 2e). This conclusion seems controversial, and may be a consequence of our selection of the objects (we will consider this in more detail below). We can only suggest that the central color indices of the disks depend on the galaxy type (see below).

Figures 3a, 3b present the dependence between the central disk color indices $(B-V)^0_{0,i}$ and $(V-I)^0_{0,i}$ and the galaxy type. The centers of the disks are redder in early-type than in late-type galaxies: $(B-V)^0_{0,i} \sim (-0.02 \pm 0.01)T$ for all three samples (correlation coefficients $|r| = 0.26, 0.29$ and 0.96 for the samples of 392, 144, and 9 galaxies, respectively) and $(V-I)^0_{0,i} \sim (-0.070 \pm 0.015)T$ for the samples of 392 and 144 galaxies, with $|r| = 0.11$ and 0.40, respectively (the dependence was weaker for the sample of 9 galaxies: $(V-I)^0_{0,i} \sim (-0.025 \pm 0.015)T$, $|r| = 0.60$). Similar dependences are derived for the other color indices, with the exception of $J-H$ and $H-K$.

The color indices at the disk edges (at a distance R_{25} from the center of the galaxy), calcu-

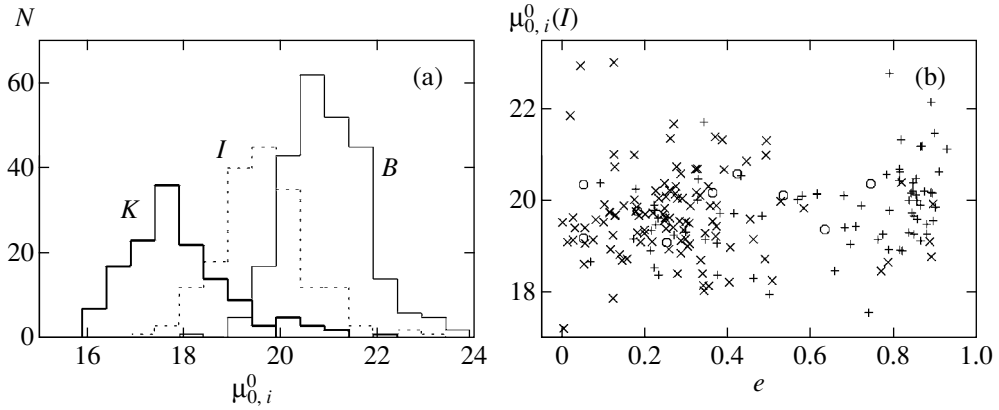

Fig. 1. (a) Distribution of the central surface brightnesses $\mu^0_{0,i}$ of the galactic disks in B (thin solid curve), I (dashed curve), and K (bold solid curve). (b) Dependence between the central surface brightness $\mu^0_{0,i}(I)$ and isophote ellipticity e of the disks. Circles mark objects from the sample of 9 galaxies, diagonal crosses those from the sub-sample of 144 galaxies, and the vertical crosses the remaining objects from the sample of 392 galaxies.

lated using the formula $(X-Y)^{R_{25}}_{0,i} = (X-Y)^0_{0,i} + 1.086R_{25}[1/h(X) - 1/h(Y)]$, show the same dependence on the galaxy type as the disk centers: $(B-V)^{R_{25}}_{0,i} \sim (-0.02 \pm 0.01)T$ (Fig. 3c). This dependence is the same for all three samples of galaxies, but, the correlation coefficients are low: only for the sample of 9 galaxies is $|r| = 0.70$, while $|r| < 0.2$ for the two other samples. Thus, it appears that the radial gradient of the disk color $\Delta(B-V)_{0,i} = (B-V)^{R_{25}}_{0,i} - (B-V)^0_{0,i}$ does not depend on the morphological type of the galaxy (Fig. 3d): most disks in galaxies of any type become bluer towards their periphery.

No correlation was found between the color indices of the disks and the luminosity and inclination of their galaxies.

3.2. Two-color Diagrams

Two-color diagrams may help us qualitatively estimate the composition of the stellar population of the disks, as well as study the star-formation history and the impact of dust in the disks (Figs. 4a, 4b). Despite the large scatter, the points indicating the color indices of the disks are concentrated towards the normal color sequence (NCS) for the integrated colors of galaxies. Radial variations of the disk color indices also occur along the NCS. The NCS curve in the diagrams is the locus for color indices of old stellar systems with exponentially decaying star formation; the smaller the color indices, the higher the star-formation rate. As we can see from Figs. 4a, 4b, most galactic disks have a standard stellar population (with NCS color indices), whose average photometric age decreases with distance from the galactic center.

Deviations of the data from the NCS indicate either a young age for the stellar population (i.e., an absence or deficit of first-generation stars in the system), or a recent burst of star formation. We studied radial variations in the stellar populations in the disks using the parameter α—the slope of the straight line characterizing the radial variations of the disk color indices. In particular, $\tan\alpha_{UBV} = \Delta(U-B)/\Delta(B-V)$ and $\tan\alpha_{BVI} = \Delta(B-V)/\Delta(V-I)$. For the normal color sequence, $\alpha_{UBV} = 55°$ and $\alpha_{BVI} = 45°$. The larger the difference $\alpha - \alpha_{\rm NCS}$ for a disk, the larger the extent to which its stellar population differs from the standard population with increasing distance from the center of the galaxy. Figures 4c, 4d present the dependences of α_{UBV} and α_{BVI} on the morphological type of the galaxy. Although the data display a large scatter, the average α is close to $\alpha_{\rm NCS}$: $\langle\alpha_{UBV}\rangle = 48° \pm 17°$ for the samples of 392 and 144 galaxies (observations in U were carried out only in [5]), and $57° \pm 33°$ for the sample of 9 galaxies; the corresponding α_{BVI} are $41° \pm 25°$, $39° \pm 27°$, and $42° \pm 21°$. While it follows from Fig. 4d that α_{BVI} is independent of the galaxy type, Fig. 4c displays some correlation: α_{UBV} decreases from early- to late-type galaxies. The typical α_{UBV} values for many late-type spiral galaxies (Sb–Sc) are $10° - 40°$. According to model calculations (see, for example, [15]), this provides evidence for an appreciable gradient of the average photometric age of the stars in the disk: the radiation from the young stellar population suppresses that from the old population at the disk peripheries.

The interpretation of the results derived from $(U-B)_{0,i} - (B-V)_{0,i}$ and $(B-V)_{0,i} - (V-I)_{0,i}$ two-color diagrams can be ambiguous, since variations of the metallicity/stellar ages and selective absorption

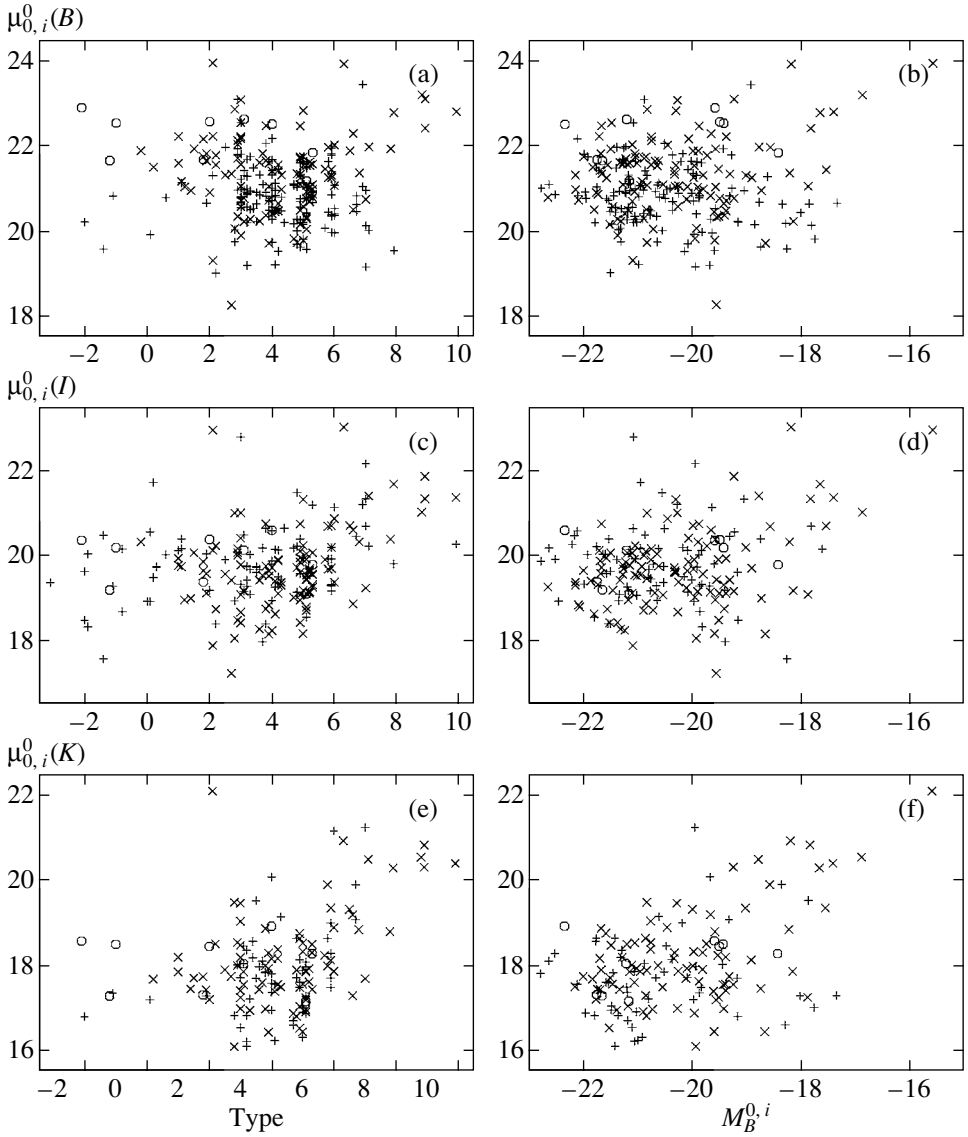

Fig. 2. The central disk surface brightnesses $\mu^0_{0,i}$ in B (a, b), I (c, d), and K (e, f) as a function of the type (a, c, e) and absolute magnitude $M^{0,i}_B$ (b, d, f) of the galaxy. The notation is the same as in Fig. 1b.

by dust both shift the points in the same direction—along the NCS. Two-color diagrams with IR color indices can be used to discriminate between the effects of dust and age or chemical-composition variations. Figure 5 presents the $(B-H)_{0,i}-(J-K)_{0,i}$ diagram for the galaxies. According to the models of [21], variations of the age of the stellar population primarily affect $B-H$, while variations of the metallicity and absorption by dust primarily affect $J-K$ (Fig. 5). Unfortunately, the photometric parameters of the disks have never been studied simultaneously in the $BJHK$ bands, so that we can apply this test only to the 9 galaxies observed by us. Note that the straight-line sections characterizing the radial variations of the disk color indices are appreciably shorter for the S0–Sa galaxies than for the spiral galaxies (Fig. 5). This provides evidence for small radial variations in the stellar population and a weak influence of dust in lenticular galaxies. In the intermediate-type S0-a galaxy NGC 7280, however, we observe a decrease in the average age of the disk stellar population with distance from the center of the galaxy, as is typical for spiral galaxies. All the spiral galaxies (with the exception of NGC 5351) display strong radial gradients of their metallicities; it is also possible that absorption by dust increases with distance from the center. In late-type (Sbc–Scd) spiral galaxies, the average age of the disk stellar population also

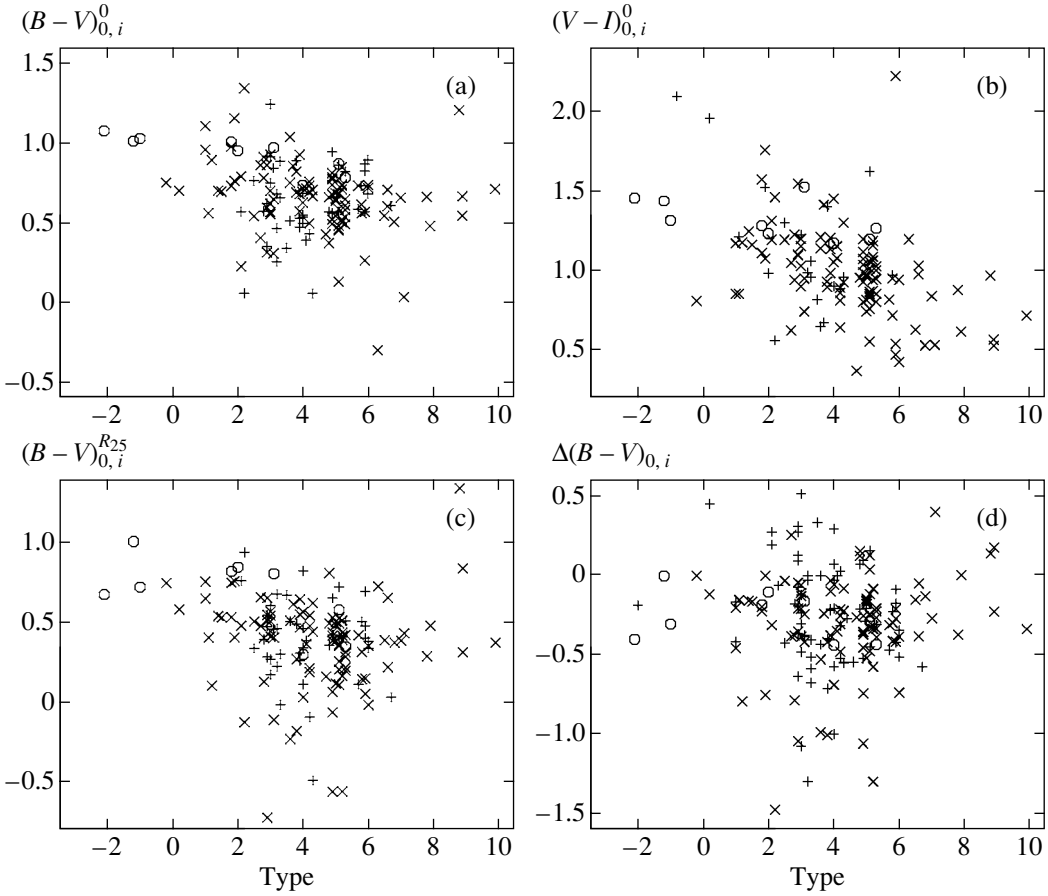

Fig. 3. The central disk color indices (a) $(B-V)^0_{0,i}$ and (b) $(V-I)^0_{0,i}$, (c) $(B-V)^{R_{25}}_{0,i}$ color indices at the disk edges, and (d) radial $\Delta(B-V)_{0,i}$ color gradient as functions of the galaxy type. Notation is the same as in Fig. 1b.

typically decreases, and the lower the average age of the disk, the larger the gradient for the decrease in age from the center to the edge of the galaxy. Here, the exception is the galaxy NGC 2336, which has a relatively young stellar population, whose age does not vary with distance from the center of the galaxy.

3.3. Absolute and Relative Size of the Disks

Both the absolute and relative sizes of the galactic disks lie in even narrower intervals than those for the central surface brightness (Figs. 6a, 6b). For the vast majority of galaxies, the absolute length scales for the disks are 2–7 kpc, while their relative scales are $h/R_{25} = 0.20-0.40$. Table 4 presents the average h and h/R_{25} values measured in various photometric bands. Note that the scatter in h and h/R_{25} substantially exceeds the difference between the absolute and relative disk scales measured in different filters (except for the shortest-wavelength U and B bands). On average, the measured h and h/R_{25} values decrease from short wavelengths (U) to long wavelengths (K). However, the disk linear sizes $h(J)$ and $h(H)$ are systematically smaller than $h(K)$. This is probably due to the fact that the IR color indices $J-H$ and $H-K$ are insensitive to the age of the stellar population.

The linear disk scale is virtually independent of the morphological type of the galaxy. Figure 6c presents the corresponding plot of $h(I)$ vs. galaxy type; similar plots are obtained for the h values for the other photometric bands. Any variation of $h(I)$ with galaxy type is substantially smaller than the range of $h(I)$ for each given morphological type. Note that the $h(I)$ range in S0 and Sd–Irr galaxies is half that in spiral galaxies: 1–6 kpc vs. 1–12 kpc (Fig. 6c). With only one exception, the linear scales for the disk brightness decreases in S0 galaxies do not exceed 5 kpc; note that our sample contains S0 galaxies with both moderate and high (for example, NGC 524) luminosities.

The plot of $h(I)/R_{25}$ as a function of the galaxy type (Fig. 6d) appears more informative than the plot in Fig. 6c. Clearly, the later the morphological

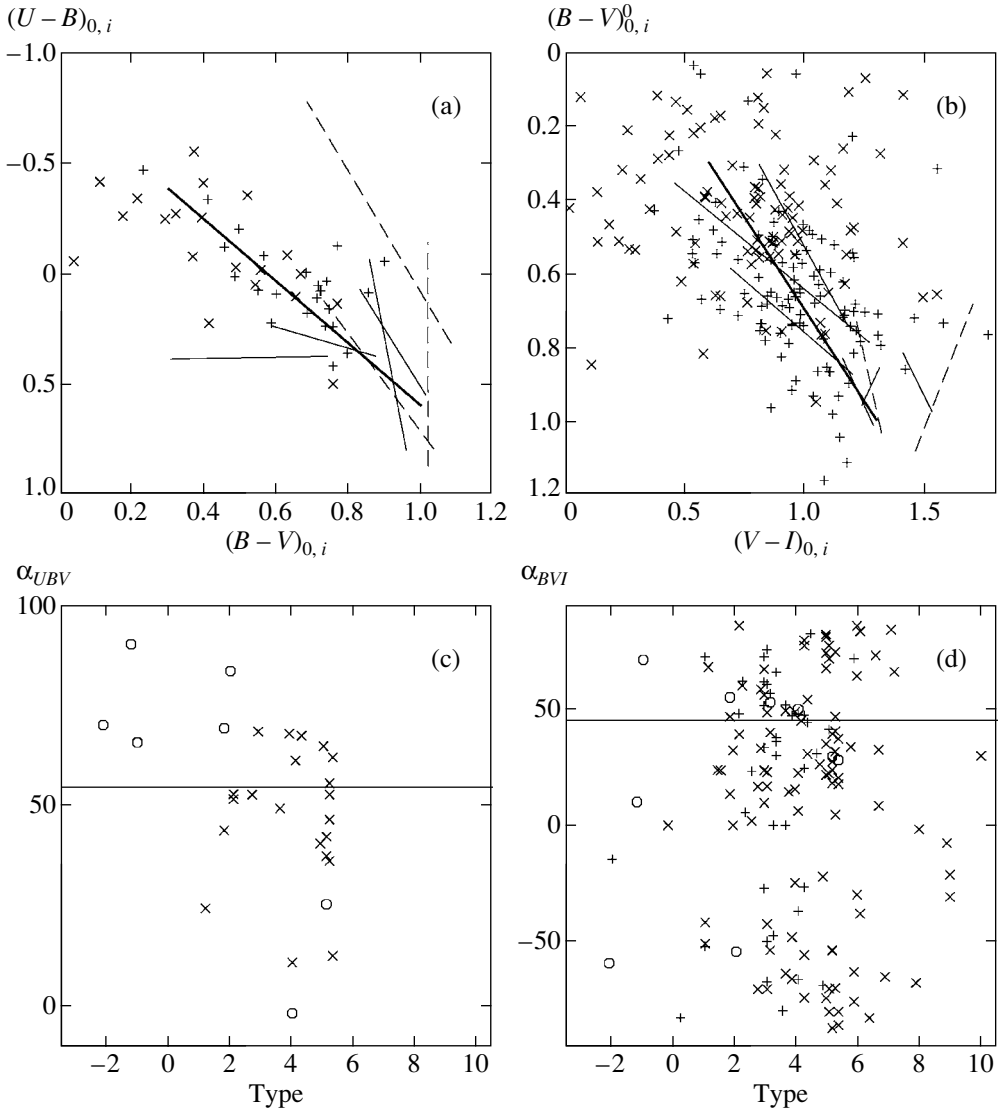

Fig. 4. (a) $(U-B)_{0,i}-(B-V)_{0,i}$ and (b) $(B-V)_{0,i}-(V-I)_{0,i}$ two-color diagrams for the galactic disks and the parameters (c) α_{UBV} and (d) α_{BVI} as functions of the galaxy type. The vertical crosses correspond to the colors at the disk centers, the diagonal crosses to the colors at the disk edges (for objects from the sample of 392 galaxies), and the circles to objects from the sample of 9 galaxies. In plots (a) and (b), the bold solid curves represent the NCS according to [20], the thin solid curves indicate the radial color variations in the disks of spiral galaxies, and the dashed curves the radial color variations in the disks of S0 galaxies (for objects from the sample of 9 galaxies). The horizontal lines in Figs. 4c, 4d correspond to $\alpha_{\rm NCS}$.

type of the galaxy, the larger, on average, the relative size of its disk. For S0 galaxies, $h(I)/R_{25}\approx 0.15-0.20$, while for Sd–Irr galaxies, $h(I)/R_{25}\approx 0.35-0.40$. Similar dependences are obtained for the relative disk sizes measured in the other photometric bands.

Thus, for the studied sample of galaxies, the relative disk size increases, the disk color becomes bluer, and the central disk K surface brightness decreases in the transition from earlier to later morphological types.

3.4. Ratio of Linear Disk Scales in Various Photometric Bands

The parameter $h(X)/h(Y)$, where X and Y are different photometric bands, is most sensitive to the presence of dust, and the dependence of $h(X)/h(Y)$ on the isophote ellipticity e forms the basic observational data for determining the parameters of dust disks in galaxies [10]. Table 5 presents the average $h(X)/h(Y)$ for our samples of galaxies.

It was shown in the Introduction that the average disk-scale ratios obtained by different authors

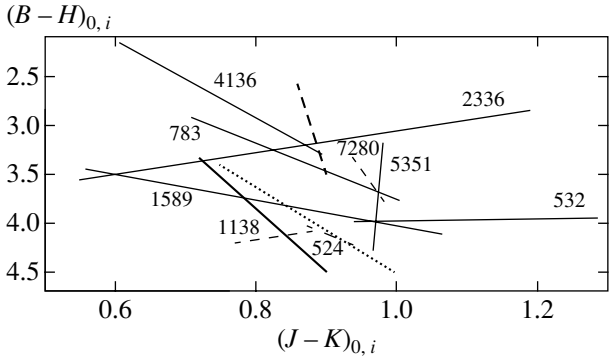

Fig. 5. $(B-H)_{0,i}-(J-K)_{0,i}$ two-color diagram for the disks. The bold solid curve indicates the displacement of the points due to absorption by dust, by $A_V = 1.0^m$ up and to the left. The dotted curve shows the metallicity gradient for a stellar system with an age of 10 Gyrs (according to [21]). The bold dashed curve represents the displacement of the points in the case of a burst of star formation [21]. Systems with higher metallicity display higher $J-K$ color indices. The thin solid and dashed curves indicate the same as those in Figs. 4a, 4b. The NGC numbers of the galaxies are marked in the graph.

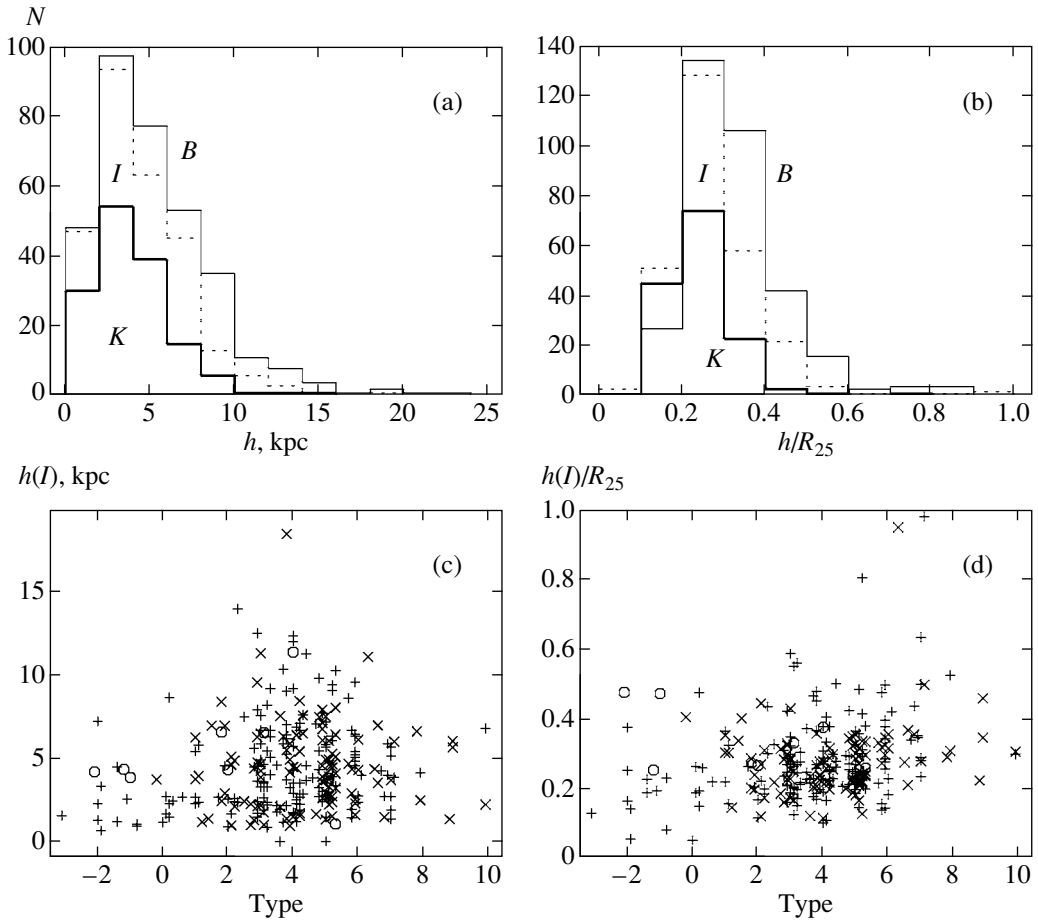

Fig. 6. Distribution of the (a) absolute h and (b) relative h/R_{25} radial scales for the brightness decreases in the galactic disks in B (thin solid curve), I (dashed curve), and K (bold solid curve), and the dependence of the (c) absolute and (d) relative sizes of the disk on the galaxy type. The notation in (c) and (d) is the same as in Fig. 1b.

differ strongly, as do the dependences of $h(X)/h(Y)$ on the isophote ellipticity e. Using the total sample, we obtained relatively small average $h(X)/h(Y)$ values (Table 5). The values for $\langle h(B)/h(I)\rangle$ and $\langle h(B)/h(K)\rangle$ agree with the estimates of [8, 14] for the case when there are appreciable effects only due

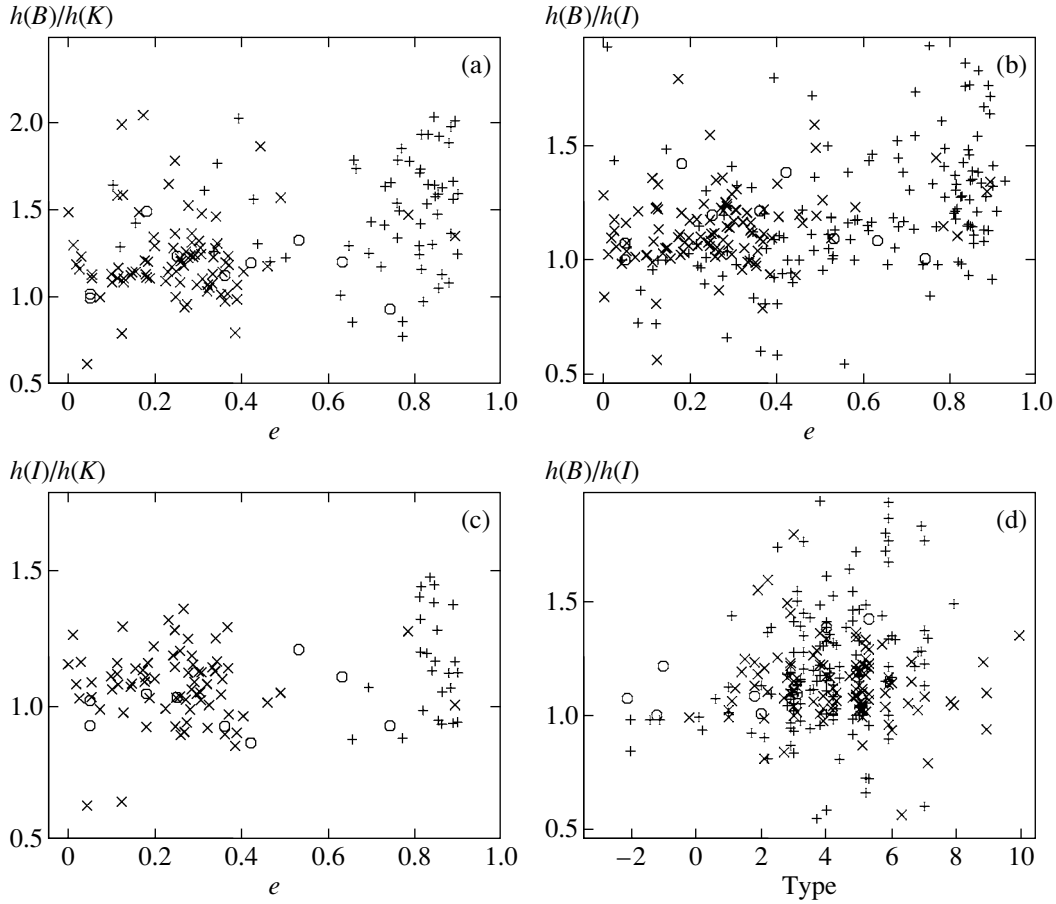

Fig. 7. Dependence of the ratios of the radial disk scales (a) $h(B)/h(K)$, (b, d) $h(B)/h(I)$, and (c) $h(I)/h(K)$ on the (a–c) isophote ellipticity e and (d) galaxy type. Notation is the same as in Fig. 1b.

to the radial age and metallicity gradients. In our opinion, the large scatter in the average $h(X)/h(Y)$ obtained in earlier studies was due to the broad interval of the observed $h(X)/h(Y)$ values (Figs. 7a, 7d).

The dependences between $h(X)/h(Y)$ and the galaxy type in the BIK bands were studied previously in [14]. The plot of $h(B)/h(I)$ as a function of the morphological type of the galaxy in Fig. 7d reproduces the results of [14]: $h(B)/h(I) = 1.0$–1.2 for S0 galaxies, the minimum value $h(B)/h(I) = 1.0$ is characteristic for all types of galaxies, and the maximum ratios increase from 1.2–1.4 for Sa galaxies to 1.6–1.9 for Sc–Sd galaxies.

Figures 7a–7c present $h(B)/h(K)$, $h(B)/h(I)$, and $h(I)/h(K)$ as functions of the ellipticity e. The ranges for the ratios of the linear disk scales are fairly large; the minimum values for $h(B)/h(K)$, $h(B)/h(I)$, and $h(I)/h(K)$ are unity independent of the inclination of the disk, while the maximum ratios increase with increasing inclination ($h(B)/h(K)$ from 1.4 to 2.0, $h(B)/h(I)$ from 1.2 to 1.8, $h(I)/h(K)$ from 1.2 to 1.4). Note that $h(I)/h(K)$ increases with the disk inclination only weakly. For the sample of 144 galaxies, we obtained the dependences $h(B)/h(I) = (1.07 \pm 0.03) + (0.24 \pm 0.09)e$ and $h(I)/h(K) = (1.07 \pm 0.03) + (0.02 \pm 0.10)e$. The fit parameters for the dependence of $h(B)/h(K)$ on e have very large errors. For the sample of 392 galaxies, the coefficients of e turned out to be systematically too large: 0.40 ± 0.08 for $h(B)/h(K)$, 0.33 ± 0.05 for $h(B)/h(I)$, and 0.12 ± 0.05 for $h(I)/h(K)$. This is due to the fact that the data for the galaxies with $e > 0.6$ were taken primarily from the three studies [1, 8, 14], which used only one-dimensional decomposition of the galaxies into bulge and disk components. The few objects with $e > 0.6$ whose disk parameters were obtained via two-dimensional decompositions display smaller $h(X)/h(Y)$ values (Figs. 7a–7c).

The correlation between $h(B)/h(I)$ and the linear disk scale length $h(I)$ noted in [10] is generally confirmed. On average, larger disks display higher $h(B)/h(I)$ ratios. However, the scatter of the data is very large: for galaxies with $h(I) \approx 1$ kpc,

Table 4. Absolute and relative disk scales

Filter	Sample of 392 galaxies	Sample of 144 galaxies	Sample of 9 galaxies
X		$h(X)$, kpc	
U	4.2 ± 2.2	4.2 ± 2.2	8.0 ± 3.7
B	5.4 ± 3.4	5.1 ± 3.4	5.9 ± 4.0
V	4.8 ± 2.9	4.6 ± 2.7	5.4 ± 3.3
R	4.8 ± 3.1	4.8 ± 3.4	5.1 ± 2.9
I	4.4 ± 2.7	4.4 ± 2.6	5.1 ± 2.8
J	–	–	4.9 ± 2.5
H	3.9 ± 1.8	3.8 ± 1.9	4.9 ± 2.9
K	4.1 ± 2.4	4.3 ± 2.4	5.2 ± 3.3
X		$h(X)/R_{25}$	
U	0.28 ± 0.09	0.28 ± 0.09	0.54 ± 0.31
B	0.33 ± 0.13	0.31 ± 0.09	0.38 ± 0.12
V	0.29 ± 0.10	0.29 ± 0.10	0.34 ± 0.09
R	0.30 ± 0.15	0.32 ± 0.19	0.33 ± 0.08
I	0.28 ± 0.13	0.28 ± 0.10	0.33 ± 0.09
J	–	–	0.33 ± 0.11
H	0.27 ± 0.12	0.29 ± 0.15	0.32 ± 0.10
K	0.25 ± 0.08	0.17 ± 0.08	0.33 ± 0.12

Table 5. Ratio of disk scales in various photometric bands

Filter	Sample of 392 galaxies	Sample of 144 galaxies	Sample of 9 galaxies
X/R		$h(X)/h(R)$	
U/R	1.18 ± 0.21	1.18 ± 0.21	1.52 ± 0.45
B/R	1.11 ± 0.15	1.09 ± 0.12	1.14 ± 0.11
V/R	1.03 ± 0.09	1.02 ± 0.06	1.04 ± 0.04
I/R	0.96 ± 0.11	0.97 ± 0.08	0.99 ± 0.07
J/R	–	–	0.98 ± 0.09
H/R	0.89 ± 0.10	0.97 ± 0.36	0.96 ± 0.08
K/R	0.87 ± 0.13	0.91 ± 0.14	0.99 ± 0.13
X/I		$h(X)/h(I)$	
U/I	1.23 ± 0.23	1.23 ± 0.23	1.51 ± 0.38
B/I	1.17 ± 0.24	1.14 ± 0.16	1.16 ± 0.15
V/I	1.07 ± 0.15	1.05 ± 0.10	1.06 ± 0.10
R/I	1.05 ± 0.12	1.03 ± 0.08	1.02 ± 0.07
J/I	–	–	0.99 ± 0.08
H/I	0.95 ± 0.10	0.95 ± 0.10	0.97 ± 0.07
K/I	0.93 ± 0.15	0.93 ± 0.17	1.01 ± 0.10
X/K		$h(X)/h(K)$	
U/K	–	–	1.51 ± 0.38
B/K	1.33 ± 0.30	1.22 ± 0.23	1.45 ± 0.32
V/K	1.13 ± 0.16	1.17 ± 0.37	1.17 ± 0.17
R/K	1.17 ± 0.18	1.14 ± 0.30	1.06 ± 0.16
I/K	1.10 ± 0.18	1.12 ± 0.32	1.02 ± 0.14
J/K	–	–	1.00 ± 0.10
H/K	0.99 ± 0.09	1.04 ± 0.33	0.97 ± 0.06

$h(B)/h(I) = 0.9$–1.4, while, for galaxies with $h(I) \approx 8$ kpc, $h(B)/h(I) = 1.0$–1.7. This dependence probably reflects the fact that both $h(I)$ and $h(B)/h(I)$, on average, increase from earlier- to later-type galaxies.

Cunow [10] constructed model grids on a plot of $h(B)/h(I)$ as a function of the ellipticity e, depending on the parameters of the dust disk τ_0 and h_{disk}/h_{dust}; the parameter $h(B)/h(I)$ characterizes radial variations in the composition of the stellar population of the disk. The $h(B)/h(I)$ values we obtained for galaxies with various e values (Fig. 7b) emcompass the entire range of models considered in [10]. Thus, the data demonstrate that, in galaxies of all types, various radial variations in the composition of the disk stellar population and a broad range of disk dust parameters are observed. We can note only a general tendency for the dust contribution and the radial gradients of the age and metallicity to increase from earlier- to later-type galaxies.

We also considered the dependence of $h(V)/h(I)$ and $h(B)/h(K)$ on the average surface density of dust $\langle\sigma_{dust}\rangle$. To this end, we used the dust masses derived in [18] from the FIR luminosities of 37 out of the 144 galaxies in our sample, as well as the dust masses for 8 galaxies whose disk parameters were determined by us (all except for NGC 1138). We calculated the average surface density of dust using the formula $\langle\sigma_{dust}\rangle = \dfrac{M_{dust}}{\pi R_{25}^2(1-e)}$; Figs. 8a, 8b present the resulting graphs. No unambiguous dependence between the disk scale ratio and the average surface density of dust can be discerned. The disks of many galaxies with large dust densities display relatively small $h(V)/h(I)$ and $h(B)/h(K)$ values (Figs. 8a, 8b). The data for 6 galaxies from our sample (all except NGC 532 and NGC 783) and for 7 galaxies with modest $\langle\sigma_{dust}\rangle$ values from the total sample yield the dependence $h(V)/h(I) = (1.00 \pm 0.04) + (3.2 \pm 1.4) \times 10^{-5}\langle\sigma_{dust}\rangle$ ($r = 0.76$),

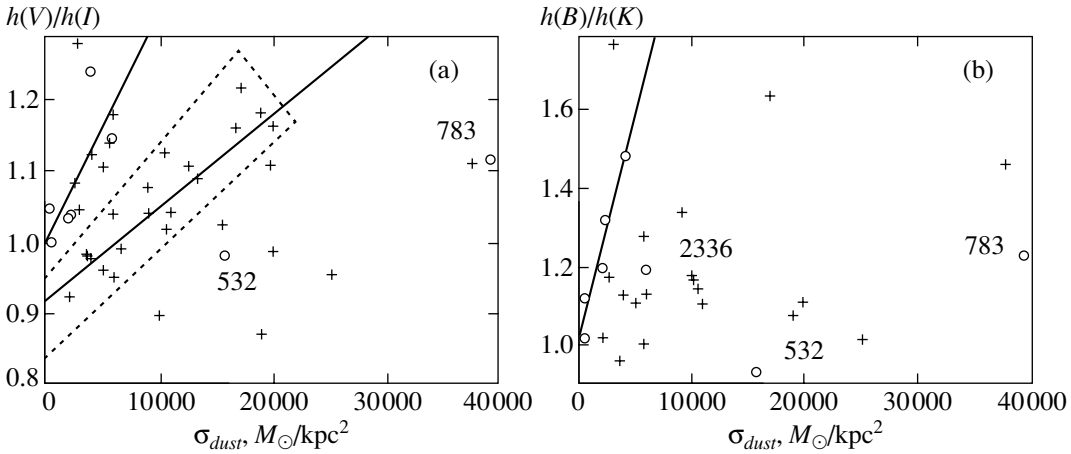

Fig. 8. Ratios of the radial disk scales (a) $h(V)/h(I)$ and (b) $h(B)/h(K)$ as functions of the average surface density of dust $\langle\sigma_{dust}\rangle$. The circles denote objects from the sample of 9 galaxies, and vertical crosses those from the sample of 37 galaxies. An explanation for the solid straight lines and dotted line are given in the text. The NGC numbers of the galaxies are indicated.

where the units for σ_{dust} are $M_\odot/\mathrm{kpc}^2$. Most galaxies from the total sample are consistent with the dependence $h(V)/h(I) = (0.92 \pm 0.02) + (1.3 \pm 0.1) \times 10^{-5}\langle\sigma_{dust}\rangle$, with the correlation coefficient $r = 0.94$ (Fig. 8a); such galaxies are located within the region delineated by dotted lines in the figure. $h(B)/h(K)$ is more weakly correlated with $\langle\sigma_{dust}\rangle$: using only 5 galaxies from our sample (all except NGC 532, NGC 783 and NGC 2336), we can derive the dependence $h(B)/h(K) = (1.02 \pm 0.04) + (11.6 \pm 1.8) \times 10^{-5}\langle\sigma_{dust}\rangle$, with $r = 0.96$ (Fig. 8b). Why do many galaxies with higher dust abundances display modest $h(V)/h(I)$ and $h(B)/h(K)$? We suggest that, when calculating the integrated dust mass in galaxies from observations, we cannot discriminate between dust that forms the exponential dust disk and dust that is concentrated towards the spiral arms and bars. For example, the galaxy NGC 4136, whose dust is concentrated in the disk [16], displays the highest $h(V)/h(I)$ and $h(B)/h(K)$. At the same time, NGC 532, NGC 783, and NGC 2336, which are more dust-abundant, display relatively small $h(V)/h(I)$ and $h(B)/h(K)$, due to the fact that a large fraction of their dust is concentrated in bands along the inner edges of their spiral arms [6].

3.5. Estimate of the Central Surface Density and Mass-to-Luminosity Ratio of the Disks

Classical thin exponential disks display a dependence between their central surface density σ_0, linear scale length h, and maximum disk rotational velocity V_{disk}: $\sigma_0 \approx 0.044V_{disk}^2/h$, where σ_0 is measured in $M_\odot/\mathrm{pc}^2$, V_{disk} in km/s, and h in kpc. Here, $V_{disk} = (0.6\text{–}0.8)V_{rot}$ (depending on the model for the galaxy), where V_{rot} is the maximum rotational velocity derived from observations. Thus, $\sigma_0 \approx 0.022V_{rot}^2/h$. Figures 9a and 9b present graphs of the dependence of $h(I)$ and $h(K)$ on V_{rot}, respectively.

In most galaxies, the central disk surface density lies in the range 50–500 $M_\odot/\mathrm{pc}^2$; the σ_0 values derived from the dependence of $h(K)$ on V_{rot} are distributed more densely (Fig. 9b). We can see a weak correlation between $\sigma_0(I)$, $\sigma_0(K)$, and the galaxy type: on average, earlier-type galaxies display larger σ_0 values (Figs. 9c, 9d). This is consistent with the dependence on galaxy type obtained for the central K surface brightness of the disk (Fig. 2e).

The quantities $\mu_{0,i}^0(K)$ and $\sigma_0(K)$ are fairly well correlated in galactic disks (Fig. 10a). $\sigma_0(K)$ can be estimated from $\mu_{0,i}^0(K)$ with an accuracy of $\pm 50\%$. A less clear correlation is observed when $\mu_{0,i}^0$ and σ_0 values measured in other photometric bands are considered. The data for our sample of 9 galaxies corresponds to the dependence $\log\sigma_0(K)[M_\odot/\mathrm{pc}^2] = -0.4\mu_{0,i}^0(K) + 9.5$ $(|r| = 0.30)$ or $\sigma_0(K) = 10^{0.4(23.75-\mu_{0,i}^0(K))} \approx 0.36(M/L(K))_\odot$ (Fig. 10a). However, the data for the total sample of 392 galaxies is consistent with the dependence $\log\sigma_0(K) \sim -0.225\mu_{0,i}^0(K)$, which indicates a dependence of the limiting value for the M/L ratio on $\mu_{0,i}^0$. For galaxies with high central disk surface brightnesses, $M/L \leq 0.9(M/L)_\odot$, while for those with low central disk surface brightnesses, $M/L \leq 0.15(M/L)_\odot$ (in the K band). A similar dependence between $\langle M/L(K)\rangle$ and the IR luminosity of a galaxy M_K was found in [22]: $\log(M/L(K)) \sim -0.08M_K$. The model calculations of [23] predict the dependence

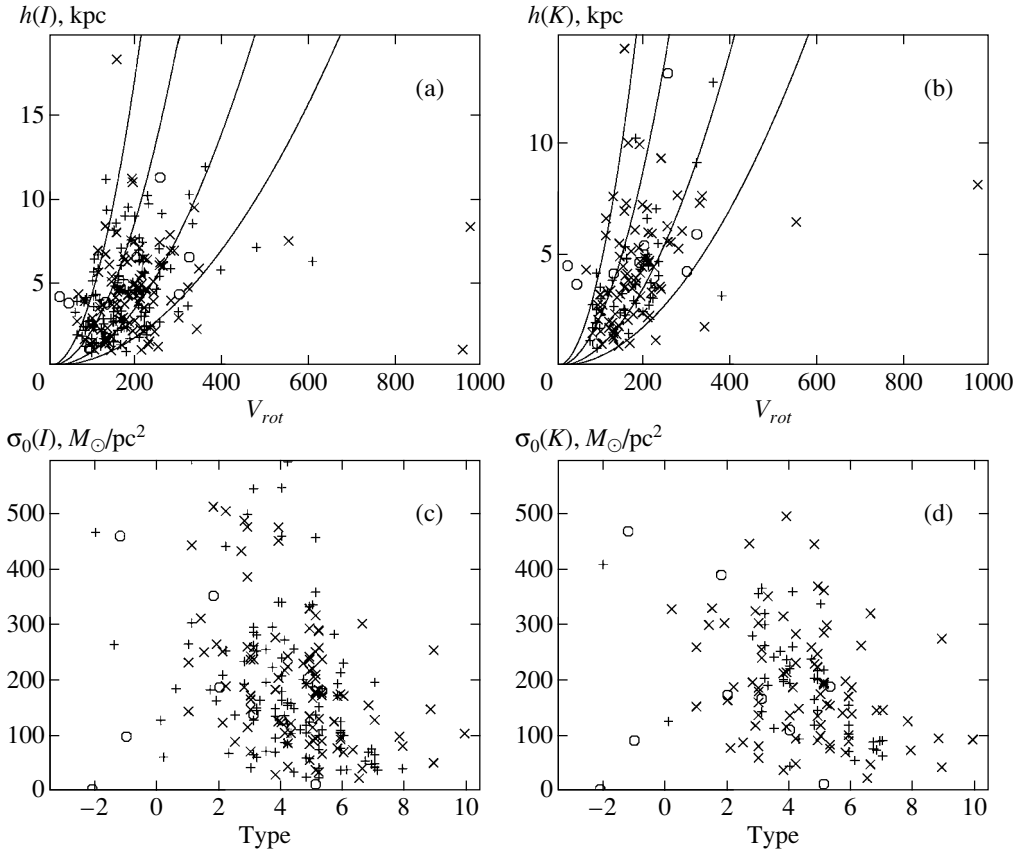

Fig. 9. Radial disk scale length h in (a) I and (b) K as a function of the maximum rotational velocity of the galaxy V_{rot}, and the dependences of the central surface density of the disk σ_0 derived from (c) $h(I)$ and (d) $h(K)$ on the galaxy type. Notation is the same as in Fig. 1b. The curves in (a) and (b) correspond to the central disk surface densities $\sigma_0 = 50, 100, 250$, and 500 $M_\odot/\mathrm{pc}^2$ (left to right).

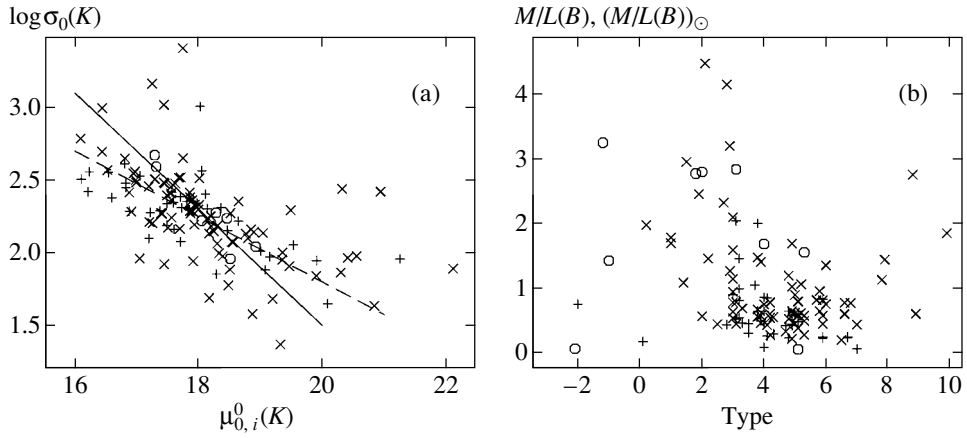

Fig. 10. (a) Logarithm of the central disk surface density $\log \sigma_0(K)$ as a function of the central surface brightness $\mu^0_{0,i}(K)$ and (b) the dependence of the ratio $M/L(B)$ at the disk center on the galaxy type. Notation is the same as in Fig. 1b. The solid line in (a) indicates the dependence for the sample of 9 galaxies, and the dotted line the dependence for the sample of 392 galaxies (see text for details).

$\log(M/L(K)) \sim -0.05\mu^0_{0,i}(K)$, where $M/L(K)$ is the mass-to-luminosity ratio for the disk as a whole and $\mu^0_{0,i}(K)$ is the central surface brightness of the stellar population of the disk. Note that the observed disk-averaged values $\langle M/L(K)\rangle$ are equal to 0.7 (according to the data of [24]) and 1.0 ± 0.4 (according to

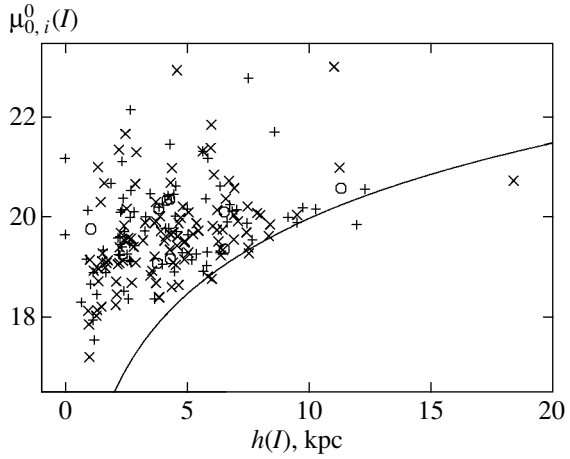

Fig. 11. Central disk surface brightness $\mu^0_{0,i}(I)$ as a function of the radial scale length $h(I)$. Notation is the same as in Fig. 1b. The curve corresponds to the total luminosity of the disk, $L(I) \approx 10^{11} L(I)_\odot$.

the data of [22]), while the model calculations of [23] predict lower values: $\langle M/L(K)\rangle = 0.5 \pm 0.2$.

We attempted to estimate the ratio $M/L(B)$ at the disk center based on the ratio of the central disk surface density $\sigma_0(K)$ and the central disk surface brightness $\mu^0_{0,i}$ in B band (Fig. 10b). This is a very indirect method for estimating $M/L(B)$, which depends strongly on the model parameters of the disk, and our results are only qualitative. As we can see in Fig. 10b, the ratio $M/L(B)$ decreases from early- to late-type galaxies. For the former, $M/L(B) = 1.5$–$3(M/L(B))_\odot$, while in most spiral galaxies, $M/L(B) = 0.3$–$1(M/L(B))_\odot$. A pronounced correlation between the maximum $M/L(B)$ values and the galaxy type is manifest by the Sb–Sd galaxies (Fig. 10b).

It is of interest how the central surface brightness of the disk $\mu^0_{0,i}(I)$ depends on its linear size $h(I)$ (Fig. 11). The distribution of galaxies in Fig. 11 displays a clear lower boundary. For galaxies with larger disks ($h(I) > 5$ kpc), this boundary reflects the limiting observed integrated luminosity of the disks $L(I) \approx 10^{11} L(I)_\odot$ (lines of equal disk luminosity correspond to the function $\mu \sim 5 \log h$ in the graph). The integrated luminosities of galaxies with moderate-size disks ($h(I) < 5$ kpc) do not reach $10^{11} L(I)_\odot$; the basic constraint here is imposed by the limiting central disk surface density ($\approx 500\ M_\odot/\mathrm{pc}^2$).

4. DISCUSSION OF THE RESULTS

The most intriguing result that we have obtained is the decrease in the central disk surface brightness in late-type galaxies in the IR, with $\mu^0_{0,i}(B)$ remaining constant along the Hubble sequence. Similar results were obtained previously by Peletier et al. [8] and de Grijs [14]. Peletier et al. [8] explained this dependence by suggesting that the centers of the galactic disks are optically thick in the B band, but optically thin in the K band. In our opinion, this interpretation leaves unexplained the dependence of $\mu^0_{0,i}(K)$ on the galaxy type, as well as the constancy of $\mu^0_{0,i}(B)$ along the Hubble sequence. If we assume that the distribution of dust corresponds to the density distribution in the stellar–gaseous disk in the galaxy, and if we consider a model with dust homogeneously mixed in a stellar–gaseous medium (which seems more correct than a dust-screen model, since the vertical scale z for the decrease of the dust-disk density is to order of magnitude equal to the vertical scale for the density of the stellar–gaseous disk [4, 10]), which yields the absorption $A_\lambda = -2.5 \log \dfrac{1 - \exp(-\tau_\lambda)}{\tau_\lambda}$, it would seem to be impossible to explain both the constancy of $\mu^0_{0,i}(B)$ and the variation of $\mu^0_{0,i}(K)$ along the Hubble sequence.

We suggest the following interpretation for the dependence of $\mu^0_{0,i}(K)$ on the galaxy type, given the constancy of $\mu^0_{0,i}(B)$. The surface brightness $\mu^0_{0,i}(K)$ at the disk center does, indeed, decrease along the Hubble sequence (at least, starting with the Sc galaxies). This is suggested by indirect but independent estimates for the central disk surface densities $\sigma_0(K)$. We assume that the volume central density of the disk ρ_0 does not depend on galaxy type, and that the variations of $\sigma_0(K)$ and $\mu^0_{0,i}(K)$ along the Hubble sequence are due to the fact that the disks of early-type galaxies are thicker (display relatively larger z values) at their centers than the disks of late-type galaxies. The main contribution to the B-band radiation is made by younger stars, whose distribution along the polar axis is approximately the same in galaxies of all types. To verify this hypothesis, supplementary observations of galaxies of different types, in particular, viewed edge-on, and studies of the $z(B)/z(K)$ dependence for the disks are needed. Note that the existence of a vertical color gradient in spiral galaxies (explained as being associated with a metallicity gradient) was discussed in [25].

Another interpretation is also possible: in late-type galaxies, the less dense disks compensate the central brightnesses with more intense star formation (i.e., giving rise to lower $M/L(B)$ values compared to those in early-type galaxies). However, this interpretation does not explain the physical origin of the constancy of $\mu^0_{0,i}(B)$.

Figure 3d shows that $\Delta(B-V)_{0,i} = (B-V)_{0,i}^{R_{25}} - (B-V)_{0,i}^{0}$ does not depend on the galaxy type. This is due to the independence of $\mu_{0,i}^{0}(B)$ on the galaxy type, and also to the way in which the parameter R_{25}—the radius of the galaxy—was determined, i.e., from the 25^m/(sq. arcsec) B isophote. Since h/R_{25} increases from early- to late-type galaxies (Fig. 6d), the color gradient normalized by the disk scale h increases along the Hubble sequence. Independently, a similar result can be derived from the dependence of $h(X)/h(Y)$ on the galaxy type (Fig. 7d) and from the two-color diagrams (Figs. 4a, 4c, 5).

The properties of dust disks and radial variations in the composition of the stellar population differ strongly in different galaxies, making it difficult to derive an unambiguous dependence between $h(X)/h(Y)$ and the isophote ellipticity e, as was done in [1]. The average $h(X)/h(Y)$ values obtained by us are consistent with the estimates made in [8, 14] for the case when the parameters are affected only by the radial gradients of the age and metallicity. Our results for the sample of 392 galaxies are fully consistent with the data of [3–5, 7, 8, 13]. Higher $\langle h(X)/h(Y)\rangle$ values were obtained in [10, 14]. The presence of dust substantially affects both $h(X)/h(Y)$ and the form of the dependence of $h(X)/h(Y)$ on the ellipticity e; however, we were not able to find any well defined correlation between the disk scale ratio and the average dust surface density, due to the fact that, while we know the total mass of dust, we cannot discriminate between dust that forms the exponential disk and dust that is concentrated toward the spiral arms and bars. The dust concentrated along spiral arms and bars does not affect $h(X)/h(Y)$.

5. CONCLUSIONS

(1) In the transition from early- to late-type galaxies, the central K surface brightness and the central surface density of the galactic disks decrease, the integrated and central color indices and central mass-to-luminosity ratio $M/L(B)$ decrease, and the relative size of the disk h/R_{25} and the ratio $h(X)/h(Y)$ increase (here, X is a shorter wavelength photometric band than Y). The color gradient (normalizing by R_{25}) and the blue central surface brightness $\mu_{0,i}^{0}(B)$ are independent of the galaxy type. The disks in early-type galaxies appear to be denser at the center and shorter than the disks in late-type galaxies. The average age of stars in the disks in early-type galaxies is higher, and the linear gradients of the age and metallicity lower than those in late-type galaxies. The impact of dust on the photometric parameters of the disks and galaxies as a whole increases in the transition to late-type galaxies.

(2) The disks in S0 galaxies have more homogeneous parameters than those in spiral galaxies. This may be due to the lower linear age and metallicity gradients of their stellar populations, as well as the lower amounts of dust in the disks of S0 galaxies. No sharp boundary in the properties of disks in lenticular, spiral, and irregular galaxies has been found—all parameters vary smoothly along the Hubble sequence.

(3) In all photometric bands, the central surface brightnesses of the disks increase with the total luminosity of the parent galaxy.

(4) The ratio of linear disk scales measured in different photometric bands $h(X)/h(Y)$ increases with the isophote ellipticity e of the disk (the inclination of the galaxy); however, the range of $h(X)/h(Y)$ values for each e value exceeds the range of variations of $h(X)/h(Y)$ over e. This is due to the fact that very broad intervals are observed for the radial variations of the composition of the stellar population in the disk and the parameters of the dust disks in the galaxies.

(5) Assuming that the surface density distribution in the disk corresponds to the K-band surface brightness distribution, the dependence $h(\sigma) = h(I)/(1.07 + 0.02e)$ can be used to determine the linear scale for the decrease of the surface density $h(\sigma)$ with an accuracy of $\pm 15\%$.

ACKNOWLEDGMENTS

The author thanks A.V. Zasov (Sternberg Astronomical Institute) for useful discussions and S.S. Kaysin (Special Astrophysical Observatory) for observations of the galaxies NGC 4136 and NGC 5351. This study was supported by the Russian Foundation for Basic Research (project nos. 04-02-16518, 05-02-16454, and 06-02-16857).

REFERENCES

1. B. Cunow, Astron. Astrophys., Suppl. Ser. **129**, 593 (1998).
2. R. E. de Souza, D. A. Gadotti, and S. dos Anjos, Astrophys. J., Suppl. Ser. **153**, 411 (2004).
3. R. S. de Jong, Astron. Astrophys., Suppl. Ser. **118**, 557 (1996).
4. E. M. Xilouris, Y. I. Byun, N. D. Kylafis, et al., Astron. Astrophys. **344**, 868 (1999).
5. C. Mollenhoff, Astron. Astrophys. **415**, 63 (2004).
6. A. S. Gusev, Astron. Zh. **83**, 195 (2006) [Astron. Rep. **50**, 182 (2006)].
7. D. M. Elmegreen and B. G. Elmegreen, Astrophys. J., Suppl. Ser. **54**, 127 (1984).
8. R. F. Peletier, E. A. Valentijn, A. F. M. Moorwood, and W. Freudling, Astron. Astrophys., Suppl. Ser. **108**, 621 (1994).

9. M. Balcells and R. F. Peletier, Astron. J. **107**, 135 (1994).
10. B. Cunow, Mon. Not. R. Astron. Soc. **323**, 130 (2001).
11. W. van Driel, E. A. Valentijn, P. R. Wesselius, and D. Kussendrager, Astron. Astrophys. **298**, L41 (1995).
12. E. Xanthopoulos, Mon. Not. R. Astron. Soc. **280**, 6 (1996).
13. L. A. MacArthur, S. Courteau, E. Bell, and J. A. Holtzman, Astrophys. J., Suppl. Ser. **152**, 175 (2004).
14. R. de Grijs, Mon. Not. R. Astron. Soc. **299**, 595 (1998).
15. A. S. Gusev and M.-G. Park, Astron. Astrophys. **410**, 117 (2003).
16. A. S. Gusev, A. V. Zasov, and S. S. Kaisin, Pis'ma Astron. Zh. **29**, 414 (2003) [Astron. Lett. **29**, 363 (2003)].
17. A. S. Gusev and S. S. Kaisin, Astron. Zh. **81**, 611 (2004) [Astron. Rep. **48**, 611 (2004)].
18. D. Bettoni, G. Galletta, and S. Garcia-Burillo, Astron. Astrophys. **405**, 5 (2003).
19. T. X. Thuan and M. Sauvage, Astron. Astrophys., Suppl. Ser. **92**, 749 (1992).
20. R. Buta and K. L. Williams, Astron. J. **109**, 543 (1995).
21. G. D. Bothun and M. D. Gregg, Astrophys. J. **350**, 73 (1990).
22. G. Moriondo, C. Giovanardi, and L. K. Hunt, Astron. Astrophys. **339**, 409 (1998).
23. E. F. Bell and R. S. de Jong, Astrophys. J. **550**, 212 (2001).
24. P. J. Grosbol and P. A. Patsis, Astron. Astrophys. **336**, 840 (1998).
25. R. F. Peletier and R. de Grijs, Mon. Not. R. Astron. Soc. **300**, L3 (1998).

Translated by K. Maslennikov